Fibers and Polymers 2012, Vol.13, No.6, 754-761 DOI 10.1007/s12221-012-0754-z

Preparation, Structure, and *in vitro* Degradation Behavior of the Electrospun Poly(lactide-co-glycolide) Ultrafine Fibrous Vascular Scaffold

Shudong Wang[1,2,3]* and Youzhu Zhang[2]

[1]*Department of Textile Engineering, College of Yancheng Textile Vocational Technology, Yancheng, China*
[2]*College of Textile and Clothing Engineering, Suzhou University, Suzhou, China*
[3]*Jiangsu R&D Center of the Ecological Textile Engineering & Technology, College of Yancheng Textile Vocational Technology, Yancheng, China*

(Received July 1, 2011; Revised January 19, 2012; Accepted January 23, 2012)

Abstract: The PLGA ultrafine fibrous scaffold was successfully fabricated by electrospinning. The morphology and properties of the PLGA vascular scaffolds were examined. In particular, the *in vitro* degradation behavior of the electrospun PLGA vascular scaffolds was investigated by means of morphology, microstructure, mass loss, M_w, and breaking strength characterization. The results showed that electrospun scaffold possessed ultrafine fibrous and porous structure, and had adequate mechanical properties to be developed as a substitute for native blood vessels. *In vitro* degradation study showed that the PLGA ultrafine fibrous scaffold could biodegrade in the PBS solution, and the mass loss, M_w, and breaking strength studies indicated that degradation rate of the electrospun PLGA nanofibers was greater in the first 2 weeks. After the degradation of 2 weeks, the degradation slowed down. Furthermore, with the extension of the degradation time, the thermal decomposition temperature of the PLGA scaffold decreased gradually. The results indicated that the electrospun PLGA vascular scaffold could be considered as an ideal candidate for tissue-engineered blood vessel.

Keywords: Electrospinning, PLGA, Degradation, Vascular

Introduction

Electrospinning has been paid much attention to as it can prepare nano-scale fibers with an extremely large surface-to-volume and high porosity. Moreover, the composition and structure can be controlled to achieve desired properties and functionality. Electrospinning has been widely applied in biomedical areas, such as nerve guidance conduit, wound dressing, bone regeneration, and vascular graft [1-4]. However, few studies have concentrated on vascular scaffolds that were fabricated by electrospinning.

The composition has a great impact on the morphological, mechanical, and biological properties of the electrospun scaffold. Poly(lactide-co-glycolide) (PLGA), the random copolymer of lactic acid and glycolic acid, has been widely used for tissue engineering applications [5,6]. Many researchers have recently studied the possibility of using PLGA as one of the candidate materials for biomedical applications because it has several useful advantages like good biocompatibility, ideal degradation behavior, good oxygen and water vapor permeability, and minimal inflammatory reaction [7,8]. In addition, the usage, especially the degradation of the PLGA, could be regulated by changing the component of lactic acid (LA) and glycolic acid (GA). A higher amount of lactic acid in the copolymer composition has better mechanical strength and longer duration of degradation [9]. However, increasing amount of lactic acid in the copolymer composition may lead to increased hydrophobicity which influences protein adsorption and subsequent cell adhesion ability [10,11].

As biomaterials, the scaffolds would degrade gradually in the body, so it is necessary to investigate the degradation behavior and degradation mechanism of the scaffolds. For example, a study by Holy *et al.* [12] investigated the degradation behavior of PLGA (75/25) porous foam in phosphate buffered saline (PBS) solution with different pH values. Yoshioka *et al.* [13] prepared the PLGA (75/25) sponges which were applied to bone tissue engineering scaffolds, and studied the mass loss and change of the morphology during the *in vitro* degradation process. Lu *et al.* [14] fabricated the PLGA (85/15 and 50/50) porous foam by means of solvent-casting, particulate-leaching technique, and researched the degradation regulation of the scaffolds with different porosity. However, there were no reports on electrospun PLGA ultrafine fibrous vascular scaffolds and the degradation behavior of the electrospun PLGA vascular scaffolds have been issued till now.

In this paper, the PLGA (75/25) ultrafine fibrous vascular scaffolds were fabricated by electrospinning using a rotating mandrel-type collector (inner diameter=6 mm). The morphology, structure, and properties of the PLGA vascular scaffolds were examined. In particular, the *in vitro* degradation behavior of the electrospun PLGA vascular scaffolds was investigated in detail. The mass, relative molecular weight, break strength, morphology, and microstructure of the PLGA vascular scaffolds before and after degradation were used to characterize the degradation behavior of the scaffolds. The results show that the electrospun PLGA vascular scaffold is an appropriate candidate for tissue engineering blood vessel.

*Corresponding author: sdwang1983@163.com

Experimental

Materials

PLGA (LA:GA=75:25) with M_w 1.1×10^5 was purchased from Daigang Co., Jinan, China. Chloroform, acetone (solvents used for electrospinning), and all the other reagents were obtained from Shanghai Chemistry Reagent Co., Shanghai, China. All of the reagents were of analytical grade.

Preparation of the PLGA Ultrafine Fibrous Vascular Scaffolds

PLGA was dissolved in a mixed solvent of chloroform and acetone (2:1 volume ratio) to obtain spinning solution with 5-9 wt.% concentrations. For electrospinning, a high electric potential was applied to a droplet of solution at the tip (ID 0.8 mm) of a syringe needle in a horizontal mount. The electrospun nanofibers were collected on a rotating mandrel-type collector with a cathode. Figure 1 shows the schematic illustration of the electrospinning setup. The spinning conditions were set as follows (listed in the order of voltage, polar distance, flow rate, and mandrel rotating speed): 25 kV, 15 cm, 0.1 m*l*/h, and 1000 rpm. The treatment process was carried out by immersing the air dried PLGA vascular scaffold in ethanol for 15 min. After ethanol treatment, the sample was exposed in a fume hood for 2 h followed by a post-treatment at 50 °C for 1 h to remove residual ethanol.

In vitro Degradation

Electrospun PLGA vascular scaffold was cut into 30×15×0.5 mm^3 samples, and then was then immersed in 10 m*l* of phosphate buffer solution (PBS) (pH=7.4) and was hydrolyzed under shaking at 60 rpm at 37 °C. After each degradation period (2, 4, 6, 8, and 10 weeks), the sample was washed and dried in a vacuum freeze-dryer for 48 h. The morphology, microstructure, strength, molecular weight, and mass loss of hydrolyzed scaffolds were examined to characterize the degradation.

Characterization of the PLGA Ultrafine Fibrous Vascular Scaffolds

Morphology

The electrospun scaffolds were observed under a scanning electron microscope (SEM; Model S-4700, Hitachi Co. Ltd., Japan). The SEM images were analyzed with Adobe Photoshop 7.0 to determine average fiber diameters. One hundred random fibers per image were used to calculate the mean and standard deviation of fiber diameters. In order to observe the morphologies of pore and calculate the pore size, the pores were determined depending on the color scale formed by an image analysis program (Imagetool 3.0) according to the color difference. The color scales which ranged from 0-255 were divided into three parts. The first part is the low scales, which stand for the micro pores, namely the blank parts. The second part is the high scales, which stand for the fibers on the surface. The third part is the medium scales, which stand for the medium fiber layers. The area of the pores were calculated and then normalized to a circular area according to the methods described by Vaz *et al.* [15] and the circular diameter was regarded as the pore diameter. The porosity of the scaffold was also calculated according to the method described by Vaz *et al.* [15]. In simple terms, the porosity (ε) was calculated with the measured average density of the samples and the standard density of PLGA (ρ_0=1.22 g/cm^3) [16], as shown in the following formula:

$$\varepsilon\,(\%) = \left(1 - \frac{\rho}{\rho_0}\right) \times 100$$

ρ stands for the average density and ρ_0 stands for standard density.

Mechanical Properties

The tensile properties of the scaffolds were characterized with an Instron tensile tester (Model 3365, Issaquah, WA, USA) in ambient conditions (20 °C and 70 % humidity). The strips [15,17,18] (30×15×0.5 mm^3), which were cut from the tubes, were measured in tension with a crosshead speed of 15 mm/min by the Instron tensile tester. Gauge length was set at 15 mm and a load cell of 100 N was used. Breaking strength, elongation, and young's modulus at break were calculated based on the generated tensile stress-strain curves. The suture retention strength of the scaffolds was measured as described by Schaner *et al.* [19]. In brief, one end of the scaffold was fixed to the stage clamp of the Instron tensile tester and the opposite end was connected to another clamp by polypropylene suture (5-0, Ethicon Inc., Piscataway, NJ, USA). The sutures were placed in 4 quadrants 2 mm from the edge of the scaffolds. The distance between the clamps was 15 mm. The scaffolds were pulled at a crosshead speed of 15 mm/min until the suture pulled through the scaffolds. The suture retention strength, which was defined as fracture strength, was obtained. Eight measurements (4 values taken from both ends of the scaffolds sample) were averaged. The burst pressure strength of the scaffolds was measured by increasing the pressure within the scaffolds until failure occurred. A pressure pump (Merit Inc., South Jordan, Utah, USA) filled with phosphate buffered saline (PBS), was used to test the burst pressure strength. The pressure was increased

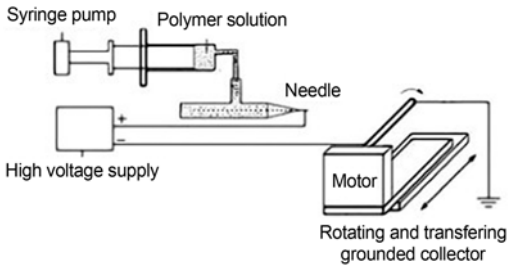

Figure 1. Schematic illustration of the electrospinning setup.

until failure or leakage occurred and then pressure change was recorded. Three samples of each material type were tested.

Microstructure

The microstructures of the vascular scaffolds before and after degradation were measured by differential scanning calorimetry (DSC) and X-ray diffraction (XRD). DSC curves were obtained by a thermal analysis instrument (Diamond, PE Co. USA) at a heating rate of 10 °C/min, a scan range of 40-400 °C and a nitrogen gas flow rate of 120 m*l*/min. The X-ray diffractions of the scaffolds were measured by a wide angle X-ray diffractometer (D/max 2027, Rigaku Co. Japan) at a scan speed of 2 °/min. The degree of crystallinity was calculated using the instrument software (Peakfit 4.12).

Mass Loss

After each degradation period (2, 4, 6, 8, and 10 weeks), the sample was dried in a oven for 30 min. The weight of PLGA vascular scaffolds before and after degradation was measured by an analytical balance. The mass loss was calculated with the following formula, three samples of each material type were tested.

$$\text{mass loss} = \left(\frac{w_0 - w_1}{w_0}\right) \times 100\%$$

w_0 and w_1 stand for the mass of the scaffolds before and after degradation respectively.

Molecular Weight Determination

The electrospun PLGA vascular scaffolds were dissolved in chloroform. The intrinsic viscosity ([η]) of PLGA and chloroform solution system was measured with an Ubbelohde viscometer. The relative molecular weight (M_w) of electrospun PLGA vascular scaffold was determined with the following formula [20]:

$$M_w = 1.8404 \times 10^5 \times [\eta]^{1.4939}$$

The drooprate of the M_w was calculated with the following formula, three samples of each material type were tested.

$$\text{drooprate of the } M_w = \left(\frac{Mw_0 - Mw_1}{Mw_0}\right) \times 100\%$$

M_{w0} and M_{w1} stand for the Mw of the PLGA scaffolds before and after degradation, respectively.

Statistical Analysis

The data was expressed as (means±standard deviations) (SD) (n=3). Statistical comparisons were performed by SPSS 13.0. *P* value is the true extent of the estimation method, and *p* value is a decline index for the credible degree. Differences were considered as significant when $p<0.05$.

Results and Discussion

Characterization of the Electrospun PLGA Vascular Scaffolds

The electrospinning parameters used for the fabrication of PLGA ultrafine fibrous vascular scaffolds were optimized by performing a series of experiments to investigate the effects of solution concentration, flow rate, voltage levels, and the distance between the syringe tip and the mandrel (see in section 2.2). Figure 2(a) and (b) showed the photograph of the whole body of the PLGA vascular scaffold, which has a length of 50 mm and an inner diameter of 6 mm with a thickness of 0.5 mm. It could be seen from Figure 2(c) that when the concentration of the solution was 7 wt.%, homogeneous, beads-free, and continuous nanofibers with average fiber diameters of (1171±295) nm (Table 1), average pore diameter of (1395±342) (Figure 2(e)) nm, and porosity of (81.8±1.4) % could be obtained. Since the as-electrospun ultrafine fibrous structure was not stable in the water or blood, the as-electrospun PLGA vascular scaffold must be treated (in the ethanol) to increase its demensional stability. Figure 3 showed the dimensional stability of the PLGA vascular scaffold before and after ethanol treatment. As shown in Figure 3(c), the inner diameter of the tubular scaffold without ethanol treatment decreased obviously when compared to Figure 3(a). However, the inner diameter of the tubular scaffold with ethanol treatment (Figure 3(b))

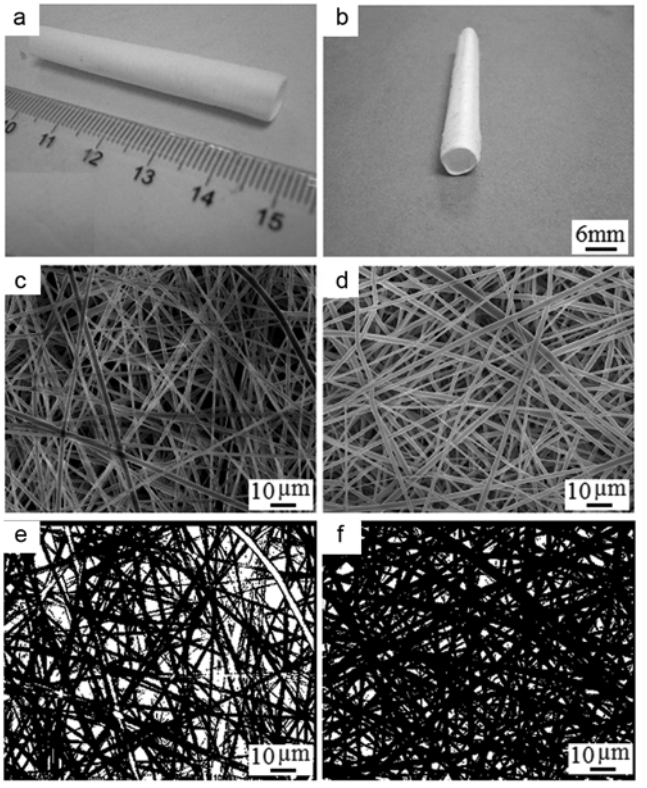

Figure 2. Macroscopic and microscopic views of the electrospun PLGA vascular scaffold. (a) and (b) whole body of the scaffold; (c) ultrafine fibrous morphology of the PLGA scaffold; (d) ethanol treated PLGA ultrafine fibrous morphology; (e) virtual images from the real SEM images of (c); (f) virtual images from the real SEM images of (d).

Table 1. Physical properties of the electrospun PLGA vascular scaffolds

Samples	Fiber diameter (nm)	Pore diameter (nm)	Porosity (%)	Breaking strength (MPa)	Elongation (%)	Young's modulus (MPa)	Suture retention strength (N)	Burst pressure strength (kPa)
As-electrospun PLGA	1171±295	1395±342	81.8±1.4	1.18±0.21	51.3±3.4	2.30±0.33	1.42±0.17	114.9±19.7
Treated PLGA	1527±189	1692±247	75.6±2.1	4.82±0.23	42.3±1.6	11.42±1.46	4.43±0.26	252.5±21.4

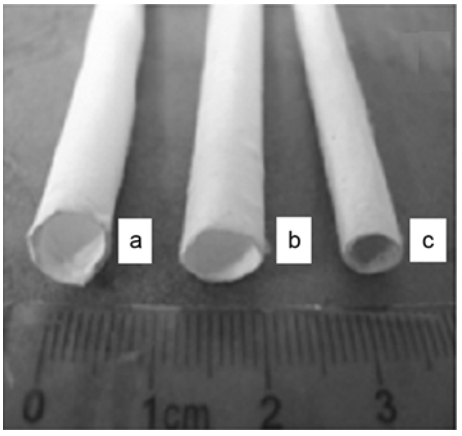

Figure 3. The morphology of PLGA vascular scaffold after immersing into the water for 10 min: (a) orginal sample, (b) ethanol treated sample, and (c) the sample without ethanol treatemnt.

kept unchanged basically when compared to Figure 3(a). Figure 2(d) and (f) showed the fibers morphology (average diameters of (1527±189) nm and average pore diameter of (1692±247) nm) of the PLGA vascular scaffold after ethanol treatment. This was due to the fiber could contract along the axial direction of the fiber, which could induce the increase of the fiber diameter and pore diameter. The preferred porosity of scaffolds used for cellular penetration should generally be within the range of 60-90 % [21]. The porous structure of the electrospun PLGA vascular scaffold mimicked the environment of the native vessel, which could provide an excellent condition for cell culture. These findings demonstrated the feasibility of using electrospinning to fabricate vascular scaffolds, as the nanoscale to microscale structure of native vessels could be mimicked by electrospinning.

Table 1 showed the mechanical properties of the PLGA vascular scaffold. As shown in Table 1, the breaking strength, elongation, and Young's modulus of the as-electrospun PLGA scaffold were (1.18±0.21) MPa, (51.3±3.4) %, and (2.30± 0.33) MPa, respectively. The ethanol treatment caused a remarkable (p<0.05) increase in breaking strength ((4.82± 0.23) MPa) and Young's modulus ((11.42±0.46) MPa), which was enhanced about 5 times higher than the as-electrospun scaffold, and the elongation decreased to (42.3±1.6) %. This was because the ethanol treatment increased the diameter of the fibers and decreased the porosity of the scaffold, which resulted in the compact structure of the PLGA scaffold. The results showed that the PLGA vascular scaffold had a desirable tensile properties for vascular grafts, which was generally accepted to be 2.0 MPa and 40.0 % [22]. Suture retention strength was a crucial factor in the fabrication of vascular scaffolds as it directly relates to the graft implantation procedure. The suture retention strength of the ethanol treated PLGA vascular scaffold ((4.43±0.26) N) evidently (p<0.05) increased compared with the as-electrospun scaffold ((1.42±0.17) N), and it was more than adequate for suturing during implantation, which was generally accepted to be greater than 2.0 N [23]. To determine whether the scaffold possessed adequate strength to endure physiologic forces, burst pressure strength was performed to identify the maximum pressure that the scaffold could endure before failure. As shown in Table 1, after ethanol treatment, the burst pressure strength of the electrospun PLGA scaffold ((252.5±21.4) kPa) increased significantly (p<0.05). Since the normal blood pressure in human body was 12.0~18.7 kPa [24], the result demonstrated that the ethanol treated PLGA vascular scaffold possessed adequate physical strength and could be developed as a substitute for native blood vessel. From the above results, the ethanol treatment dramatically improved the mechanical properties of the electrospun PLGA vascular scaffold. We assumed that a higher density of the ethanol treated PLGA scaffold may be responsible for this tremendous improvement. The density of the ethanol treated PLGA vascular scaffold was (0.29±0.02) g/cm^3, which was higher than that of the as-electrospun PLGA vascular scaffold (0.21±0.01) g/cm^3. The result induced that the mechanical properties of the electrospun PLGA vascular scaffold after ethanol treatment dramatically improved.

In vitro Degradation of the Electrospun PLGA Vascular Scaffolds

The *in vitro* degradation study involved analyzing the change in morphology, mass, molecular weight, break strength, and microstructure of the electrospun PLGA vascular scaffold during the course of degradation.

Morphology

The change in morphology of the PLGA ultrafine fibrous vascular scaffold during the process of degradation was characterized by means of SEM. Figure 4 showed the SEM images of the PLGA vascular scaffold at each degradation period. It could be seen from Figure 4 that the PLGA nanofibers were swollen after 2 weeks of degradation (Figure 4(b)) when compared to the original sample (Figure 4(a)), and the

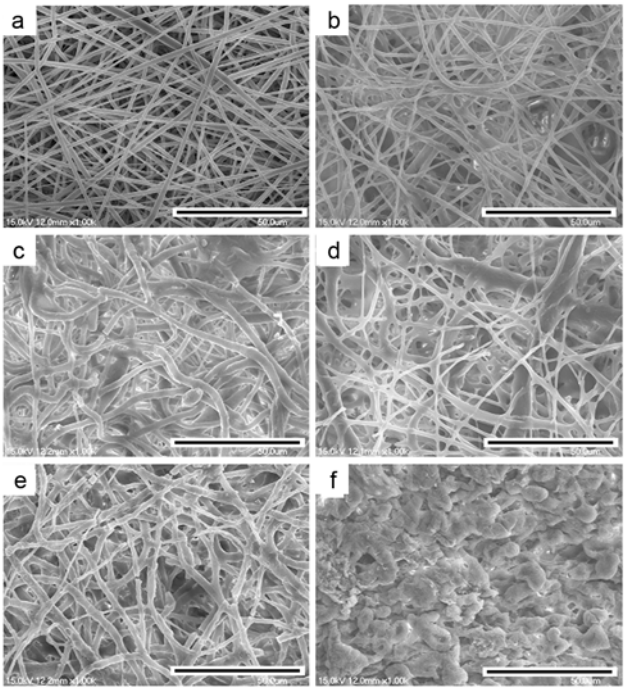

Figure 4. SEM images of the PLGA nanofibers (a) and degradation of 2 weeks (b), 4 weeks (c), 6 weeks (d), 8 weeks (e), and 10 weeks (f).

nanofibers were partially adhered to another. After 4 weeks of degradation (Figure 4(c)), the fibers were considerably swollen. The ultrafine fibrous meshes showed conglutination, and some surface defects (microcracks) were also observed. The PLGA nanofibers became rough and showed some ruptures after 6 weeks of degradation (Figure 4(d)). However, at this time, the ultrafine fibrous structure was maintained. When the degradation time reached 8 weeks, large scale of ruptures were observed (Figure 4(e)) and the PLGA ultrafine fibrous scaffold changed into chunks consisting of the short fiber fragments. After 10 weeks of degradation, the morphology of the PLGA nanofibers disappeared (Figure 4(f)), the PLGA ultrafine fibrous scaffold cracked into amounts of fragments, and the PLGA microfibrous meshes also shrunk in size as evidenced by reduction in overall dimension. From the above results and analysis, it could be concluded that the degradation rate of PLGA ultrafine fibrous scaffold was higher than that of the PLA ultrafine fibrous scaffolds [25,26]. This was due to the lower crystalline of the PLGA scaffold, the XRD patterns of PLGA and PLA were shown in Figure 5. It could be seen from Figure 5 that the PLA scaffold (Figure 5(b)) had remarkable crystalline diffraction peak, but there was not obvious crystalline peaks occurred at the PLGA scaffold. Based on the XRD patterns, the crystallinity of the PLA (78.6 %) and PLGA (17.8 %) were calculated. The crystallinity of the PLA scaffold was higher than that of the PLGA, which induced the degradation rate

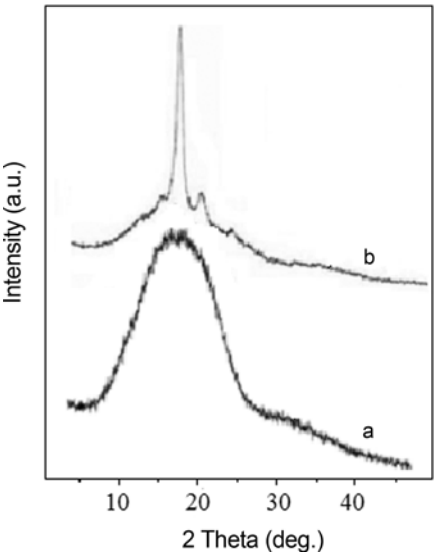

Figure 5. The XRD patterns of PLGA (a) and PLA (b) vascular scaffold.

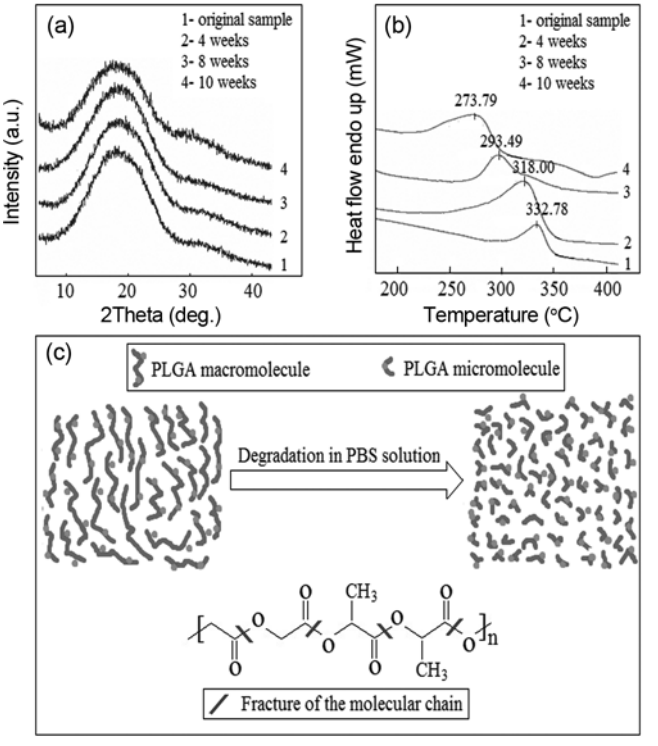

Figure 6. XRD patterns (a) and DSC curves (b) of the electrospun PLGA ultrafine fibrous vascular scaffold, and the schematic illustration of the degradation action (c).

of PLGA scaffold was higher than that of the PLA scaffold.

Microstructure

Presence of the crystalline region had a great influence on the degradation during the process of degradation. To investigate the crystal structures of the PLGA nanofibers

before and after degradation, the XRD patterns were measured for these samples. The X-ray diffractograms of the PLGA nanofibers before and after degradation were shown in Figure 6(a). As shown in Figure 6(a), the PLGA original sample (before degradation) did not show remarkable crystal diffraction peaks, which indicated that the PLGA original sample was almost amorphous polymer. Along with the degradation (4 weeks, 8 weeks, and 10 weeks), the PLGA nanofibers did not show remarkable crystal diffraction peaks as well. Based on the XRD patterns, the degrees of crystallinity of the PLGA vascular scaffolds at different degradation times were calculated. The degrees of crystallinity of the PLGA scaffold were 17.8 % (0 week), 16.8 % (4 weeks), 16.1 % (8 weeks), and 15.4 % (10 weeks) respectively. The results demonstrated that all of the electrospun PLGA ultrafine fibrous scaffolds before and after degradation had lower crystallinity, which indicated that the microstructure of the PLGA ultrafine fibrous scaffolds before and after degradation was almost amorphous structure. The results also showed the reason why the electrospun PLGA ultrafine fibrous scaffold degraded quickly in the morphology section.

The M_w and dimension of the molecular chain and the degradation could be investigated by DSC. The decrease of the M_w and dimension of the molecular chain demonstrated that the M_w decreased and the macromolecular chain of the PLGA ultrafine fibrous scaffold turned into micromolecular chain after degradation. The DSC thermograms of the PLGA ultrafine fibrous scaffold before and after 4 weeks, 8 weeks, and 10 weeks of degradation were shown in Figure 6(b). As shown in Figure 6(b), all of the PLGA scaffolds before and after degradation had a thermal decomposition peak, but the thermal decomposition temperature of each scaffold was different. The thermal decomposition temperature of the PLGA original sample was 332.78 °C, and the thermal decomposition temperature of the PLGA scaffold decreased gradually after degradation of 4 (318.00 °C), 8 (293.49 °C), and 10 weeks (273.79 °C). This was because the macromolecules were cut off by water molecule during the degradation, which induced that the M_w and intermolecular force of the PLGA nanofibers decreased. Furthermore, the macromolecular chain of the PLGA nanofibers turned to micromolecular chain after degradation, which was another reason for the decrease of the thermal decomposition temperature. And the schematic illustration of the degradation action could be illuminated in Figure 6(c).

Mass Loss and Change of the M_w

Degradation of the PLGA nanofibers was expected to cause a decrease in the physical mass of the samples. With the extension of degradation time, partial degradation products dissolved in the PBS solution and induced the decrease of mass (mass loss). The mass loss could characterize the degradation rate, and a big mass loss meant a high mass loss. The mass loss of the PLGA ultrafine fibrous vascular scaffold at each degradation time was shown in Figure 7. It

Degradation time (week)	2	4	6	8	10
Mass of the original sample (g)	0.1112	0.0651	0.02502	0.0930	0.0613
Mass of the sample after degradation (g)	0.0967	0.0542	0.1925	0.0661	0.0429
Mass loss (%)	13.04	16.70	23.06	28.91	30.01

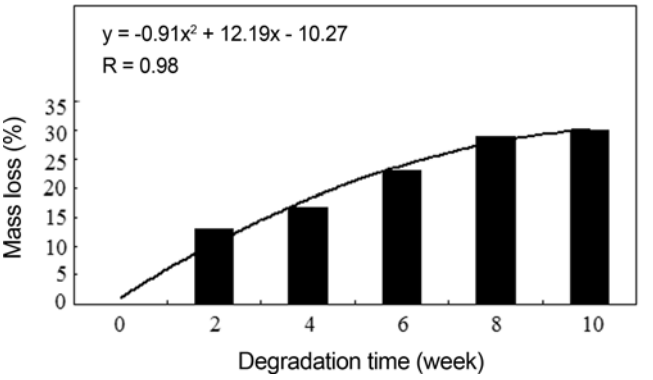

Figure 7. Mass loss of the electrospun PLGA ultrafine fibrous vascular scaffold during the process of degradation.

could be seen from Figure 7 that the PLGA ultrafine fibrous vascular scaffold demonstrated a greater mass loss in the first two weeks of degradation and the mass loss of the scaffold reached 13.04 %. With the extension of degradation time, the mass loss of the PLGA vascular scaffold increased gradually. However, the speed of increasing slowed down. The increase of the mass loss was about 16 % from 2 weeks of degradation to 8 weeks of degradation, and it was only less than 2 % from 8 weeks of degradation to 10 weeks of degradation. This was because the glycolic acid (GA) was a relative hydrophilic component, and it could swell quickly in the PBS solution. The PLGA molecular chain ruptured preferentially at the ester bond in the GA-GA or GA-lactic acid (LA). And it caused the GA component hydrolyzed quickly, so the mass loss in the first two weeks of degradation was greater. After the degradation of the GA component, most of the residual components of the PLGA nanofibers were LA. The degradation rate of the LA component was relatively slower when compared to the GA component, and it explained why the degradation slowed down during the degradation time from 4 weeks to 10 weeks.

The mass loss study only provided a physical evidence for degradation of the PLGA ultrafine fibrous vascular scaffold. However, in order to understand the process at the molecular level, M_w of the PLGA ultrafine fibrous scaffold was analyzed for the entire duration of the degradation. The change of the M_w in the process of the degradation was shown in Figure 8. As shown in Figure 8, the M_w of the PLGA original sample was 110333, and the M_w decreased with the extension of degradation time, which demonstrated that the electrospun PLGA nanofiber was biodegradable polymer. It could also be seen from Figure 8 that the drooprate

Degradation time (week)	0	2	4	6	8	10
[η]	0.71	0.48	0.40	0.33	0.28	0.26
M_w	110333	61478	46818	35124	27479	24599

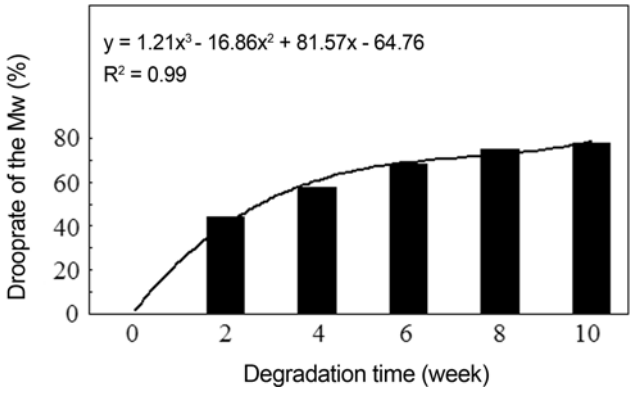

Figure 8. Change of the M_w of the PLGA ultrafine fibrous vascular scaffold with the extension of degradation.

of the M_w reached 44.28 % quickly after degradation of 2 weeks. And with the extension of degradation time, the drooprate of the M_w increased gradually. However, the speed of the decreasing slowed down. The results and the reason were in accordance with the analysis of the mass loss section.

Change of the Breaking Strength

As biodegradable material, the breaking strength of the scaffold decreased with the extension of degradation time consequentially. The degradation degree and rate could be characterized by means of breaking strength of the scaffold at different degradation times. Moreover, in order to investigate the relation between the maintenance time of the mechanical properties and the tissue regeneration time, it was necessary to investigate the breaking strength of the scaffold during each degradation time, and the results were shown in Figure 9. As shown in Figure 9, the drooprate of the breaking strength reached (36.8±1.4) % quickly after the degradation of 2 weeks. This was due to the fact that the macromolecular chain was cut off quickly by the water molecule, and the intermolecular force of the PLGA nanofibers decreased, and induced the decrease of the breaking strength. After the degradation of 4, 6, and 8 weeks, the drooprate of the breaking strength increased significantly ($p<0.05$). However, the speed of the decreasing slowed down. The results and reason were in accord with the mass loss and change of the Mw section. After 10 weeks of degradation, the PLGA ultrafine fibrous scaffold cracked into amounts of fragments, and the PLGA ultrafine fibrous scaffold lost the mechanical properties. It may be concluded that the breaking strength of the PLGA strength could be controlled by regulating and controlling the degradation time and the proportion of the GA and LA component. We would take this research in the future work.

Degradation time (week)	2	4	6	8
Breaking strength of the original sample (MPa)	4.83±0.19	4.72±0.15	4.59±0.21	5.12±0.13
Breaking strength of the samples after degradation (MPa)	3.05±0.14	3.29±0.18	2.33±0.16	2.11±0.15
Drooprate (%)	36.8±1.4	43.1±1.9	49.2±2.2	58.8±1.6

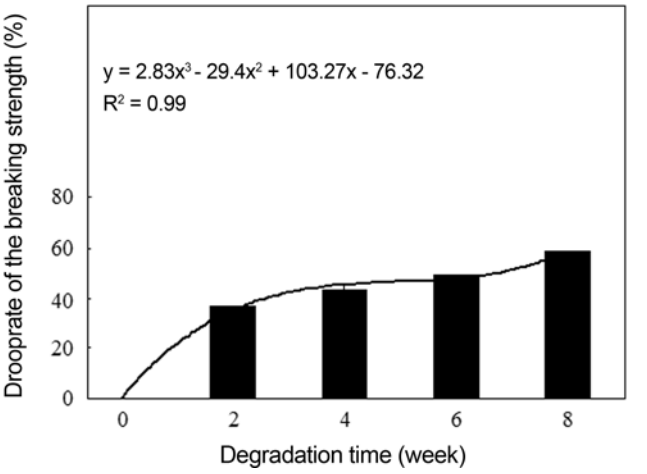

Figure 9. Change of the breaking strength of the PLGA ultrafine fibrous vascular scaffold with the extension of degradation.

Conclusion

In the present study, a PLGA ultrafine fibrous scaffold produced by electrospinning was introduced for potential use in vascular tissue engineering. The PLGA vascular scaffold (inner diameter=6 mm) with homogeneous, beads-free, and continuous nanofibers was successfully prepared by electrospinning. The tensile, suture retention, and burst pressure strength indicated that the electrospun PLGA vascular scaffold possessed adequate mechanical properties to develop as a substitute for native blood vessels. *In vitro* degradation study demonstrated that the PLGA nanofibers swell and fractured in the first few weeks. After degradation for 10 weeks, the scaffold cracked into amounts of fragments. The XRD studies showed that electrospun PLGA ultrafine fibrous scaffolds were almost amorphous structure before and after degradation. With the extension of degradation time, the thermal decomposition temperature of the PLGA scaffold decreased gradually. In addition, the mass loss, M_w, and breaking strength studies indicated that degradation rate of the electrospun PLGA nanofibers was greater in the first 2 weeks, and after degradation for 2 weeks, the degradation rate slowed down. The above results of *in vitro* degradation study showed that the PLGA ultrafine fibrous scaffold could biodegrade in the PBS solution. All the investigations demonstrated that the electrospun PLGA vascular scaffold was an appropriate candidate for tissue engineering blood vessel.

Acknowledgements

This research was supported by a grant from Jiangsu Province Key Lab Foundation of China (No. KJS0817). And we were also indebted to the Testing Center of Suzhou University and Yancheng Textile Vocational Technology College for experimental support.

References

1. S. D. Wang, Y. Z. Zhang, H. W. Wang, and Z. H. Dong, *Int. J. Biol. Macromol.*, **48**, 345 (2011).
2. J. A. Matthews, G. E. Wnek, D. G. Simpson, and G. L. Bowlin, *Biomacromolecules*, **3**, 232 (2002).
3. M. Gu, K. Wang, W. Li, C. Qin, J. Wang, and L. Dai, *Fiber. Polym.*, **12**, 65 (2011).
4. S. D. Wang, Y. Z. Zhang, G. B. Yin, H. W. Wang, and Z. H. Dong, *J. Appl. Polym. Sci.*, **113**, 2675 (2009).
5. S. J. Kim, D. H. Jang, W. H. Park, and B. M. Min, *Polymer*, **51**, 1320 (2010).
6. R. Dorati, C. Colonna, I. Genta, T. Modena, and B. Conti, *Polym. Degrad. Stab.*, **95**, 697 (2010).
7. E. A. Sander, A. M. Alb, and E. A. Nauman, *J. Biomed. Mater. Res. A*, **70**, 506 (2004).
8. V. Rajesh, S. Kirubanandan, and S. K. Dhirendra, *Polym. Degrad. Stab.*, **95**, 1605 (2010).
9. H. J. Shin, C. H. Lee, I. H. Cho, Y. J. Kim, Y. J. Lee, and I. A. Kim, *J. Biomater. Sci. Polym. Ed.*, **17**, 103 (2006).
10. E. I. Vargha-Butler, E. Kiss, C. N. C. Lam, Z. Keresztes, E. Kalman, and L. Zhang, *Colloid. Polym. Sci.*, **279**, 1160 (2001).
11. T. I. Croll, A. J. O'Connor, G. W. Stevens, and J. J. Cooper-White, *Biomacromolecules*, **5**, 463 (2004).
12. C. E. Holy, S. M. Dang, J. E. Davies, and M. S. Shoichet, *Biomaterials*, **20**, 1177 (1999).
13. T. Yoshioka, N. Kawazoe, and T. Tateishi, *Biomaterials*, **29**, 2438 (2008).
14. L. Lu, S. J. Peter, M. D. Lyman, H. L. Lai, S. M. Leite, J. A. Tamada, S. Uyama, J. P. Vacanti, R. Langer, and A. G. Mikos, *Biomaterials*, **21**, 1837 (2000).
15. C. M. Vaz, S. V. Tuij, and C. V. C. Bouten, *Acta Biomaterial*, **1**, 575 (2005).
16. S. Y. Li, S. D. Wang, Y. Z. Zhang, H. W. Wang, and P. Qiu, *Synthetic Fiber China*, **11**, 22 (2009).
17. S. Wang, Y. Zhang, H. Wang, G. Yin, and Z. Dong, *Biomacromolecules*, **10**, 2240 (2009).
18. S. J. Lee, J. Liu, S. H. Oh, S. Soker, A. Atala, and J. J. Yoo, *Biomaterials*, **29**, 2891 (2008).
19. P. J. Schaner, N. D. Martin, and T. N. Tulenko, *J. Vasc. Surg.*, **40**, 146 (2004).
20. R. P. F. Lanao, S. C. G. Leeuwenburgh, J. G. C. Wolke, and J. A. Jansen, *Acta Biomaterialia*, **7**, 3459 (2011).
21. H. M. Kim, T. Kokubo, and S. Fujibayashi, *J. Biomed. Mater. Res. A*, **52**, 553 (2000).
22. J. Stitzel, J. Liu, S. J. Lee, M. Komura, J. Berry, and S. Soker, *Biomaterials*, **27**, 1088 (2006).
23. K. Billiar, J. Murray, and D. Laude, *J. Biomed. Mater. Res. A*, **56**, 101 (2001).
24. S. D. Wang, Y. Z. Zhang, G. B. Yin, H. W. Wang, and Z. H. Dong, *Mater. Sci. Eng. C*, **30**, 670 (2010).
25. Elisabeth, R. Caroline, M. Liz, B. Jonathan, C. Mike, F. M. Aline, and S. Alberto, *Polym. Degrad. Stab.*, **93**, 1869 (2008).
26. A. M. Reed and D. K. Gilding, *Polymer*, **22**, 494 (1981).